

SUPPLEMENTARY INFORMATION

Common clonal origin of central and resident memory T cells following skin immunization

Olivier Gaide¹, Ryan O. Emerson², Xiaodong Jiang¹, Nicholas Gulati³, Suzanne Nizza¹, Cindy Desmarais², Harlan Robins⁴, James G. Krueger³, Rachael A. Clark¹ and Thomas S. Kupper¹

Supplementary Figure 1. Unbiased tracking of T cell clones and their progeny during three immunization schemes, using high-throughput TCR β sequencing. **a**, Outline of experimental plan for sampling skin and lymph node tissue for DNA extraction and TCR sequencing before and after immunization with three distinct antigenic challenges: OVA+CT, DNFB or MVA (n=3 mice for each condition, all experiments performed 2-3 times, representative data is shown). **b**, Ear swelling 1 day after the second OVA+CT immunization, DNFB immunization or 6 days after MVA infection, respectively. n=3 mice for each group. All experiments performed 2-3 times, representative data shown. **c**, Frequency (y axis) of respective V(x-axis)J(z-axis) subgroups in the spleen of 3 wild-type C57Bl/6 mice and OT-I mice, highlighting the presence of a single TCR clone in the OT-I mouse (n=4). **d**, Relative and absolute numbers of the OT-I TCR sequence measured in the LN of mice 1 day after adoptive transfer of 10^4 , 10^5 or 10^6 naive OT-I cells, showing dose-dependent abundance of the clone (n=3 mice). As a control, normal C57Bl/6 littermates that were not injected (No T) or the spleen of an OT-I mouse were analyzed (n=9 mice). **e**, Dot plots (TCR sequencing, each dot represents a unique CDR3 sequence) showing the frequency of TCR β sequences in the skin and LN of a C57Bl/6 mouse injected with 10^5 OT-I cells before (left panel, ILN vertical axis, tail skin horizontal axis) and 6 weeks after (right panel, draining

LN y axis, treated skin x axis) immunization with OVA+CT (see also figure 1). The OT-I clone CASSRANYEQYF, is present only in the LN before immunization, as naive OT-1 cells were injected one day prior, and is detected in both the skin and LN only after immunization. (n=3 mice). **f**, Dot plot of the absolute number of T cells (rather than percentage) observed in 400ng of gDNA from skin and LN, respectively, after OVA+CT immunization. Gray lines link individual clones (dots) between skin and LN, demonstrating that T cell clones are present in comparable absolute numbers in both compartments. The insert shows the number of OT-I cell clones in the spleen of an OT-I mouse, demonstrating only a single sequence (n=3 mice). **i**, Anatomic tracking of the TCR β sequences identified in (f), showing a common pattern of absolute T cell numbers in the skin and LN, both draining and distant, occurring after OVA+CT immunization. The OT-I TCR is the sole clone detected in LN prior to immunization, a result of naïve OT-I T cell injection prior to antigen exposure. Numbers in skin vs LN are similar, well within an order of magnitude, per 400ng gDNA.

Supplementary Figure 2. Peripheral TCR presence is not due to tissue contamination by blood T cells.

a, Tracking of the OT-I TCR sequence (DNA) in different mice tissues, before and after OVA+CT immunization (immunization as shown in figure 1a). The OT-I clone, 24 hour after injection in the blood stream, is not detected in the skin (pre-imm), suggesting that blood contamination of skin undetectable. After immunization, the OT-I clone can be found at the expected sites, i.e. local and distant skin sites and LN, at low levels in lung, but not in the gut or vagina. If the presence of the clone in distant skin and LN was due to contamination of the tissues by blood, it should also be observed in the gut or vagina. Detection of the clone in the lung is expected, as skin immunization is known to induce a small population of T cells with lung-migrating properties²¹. (n=3 mice). **b**, Blood vs. tissue distribution of the 10 most abundant T cell clones in blood and skin, respectively, in mice repeatedly exposed to DNFB (Fig 2). Of the 10 most prevalent T cell clones in the blood, 9 are not detected in the skin or LN (right panel).

Conversely, the most prevalent clones in the skin, which are observed at distant skin and LN sites, are either absent or underrepresented in blood (left panel). Together, these findings demonstrate that blood contamination of skin or LN was undetectable, and certainly too low to significantly alter the TCR profiling of mouse tissues. (n=3 mice).

Supplementary Figure 3. Frequency of CD4 and CD8 T cells in local and distant skin sites and LN, after multiple DNFB immunization. **a**, Sensitization and challenge scheme. Experiments performed 3 times, representative data shown. **b**, Dot plots (FACS) of CD4⁺ and CD8⁺ in the tail (not exposed), the right ear (exposed once during challenge) and left ear (exposed 4 times during immunization, boost and challenge), with a non-immunized ear skin as control (n=3 mice). **c**, Dot plots of CD4⁺ and CD8⁺ cells in the LN of immunized and non-immunized mice (n=3 mice). **d**, Ratio of CD4⁺ and CD8⁺ cells, in relation to gamma-delta + cells, in the skin of naïve and immunized skin, either non exposed, challenged once, or sensitized and challenged (n=3 mice; values are given as mean ± SD). **e**, Dot plot of skin-resident TCRβ⁺ T cells of OVA+CT immunized mice, showing a CD8⁺ and CD8⁻ (ie CD4⁺) population (memory phase) (n=3).

Supplementary Figure 4. Phenotype of CD8 T cells present in LN (T_{CM}) and skin (T_{RM}) 30 days after DNFB immunization (memory phase). **a**, Dot plots (FACS) showing the expression pattern of the indicated surface markers. The expression pattern is the same as that observed after MVA or VV vaccination, i.e. CD44^{high}, CD62^{neg}, CD69⁺, CD103^{high} CD122^{neg}, E and P-selectin high for T_{RM} (showing antigen experience and skin homing characteristics), and CD62^{pos}, CD69⁻, E and P-selectin lower for T_{CM}. Representative dot plots of 1 of 9 mice in 3 independent experiments.

Supplementary Figure 5. Activated naïve T cell clones give rise to both skin-resident T_{RM} and re-circulating T_{CM} . **a**, Experimental plan: at day -7, skin and LN biopsies were taken from two mice that would be later be joined by parabiotic surgery. One mouse was DNFB sensitized on day 0, 1, and 7, while the other was not. At day 35, these mice were surgically joined (parabiosis) and kept as pairs for 4 weeks. At day 63, mice were separated and skin (tail and ear) and LN (inguinal and cervical) were harvested for HTS (n=3 pairs of mice). Experiments were performed 2-4 times. **b**, Ear swelling 1 day after DNFB challenge in a different cohort of mice at day 35 confirming induction of T_{RM} memory to DNFB at this time point (n=6 mice for each condition). **c**, Dot plots of the frequency (number of a given sequence divided by the total number of sequences observed in the sample) of TCR β sequences found in the inguinal LN and the skin before and after parabiosis, with the sensitized mouse on the y axis, naïve mouse on the x axis. Prior to parabiosis, syngeneic mice share very few common TCR sequences (<0.5% average, 95%CI 0.3-1%). After parabiosis, the number of common sequences increases dramatically (3% average, 95%CI 2-12%). This increase is roughly equal the number of sequences common to 2 different LN of the same mouse (~3%; the insert shows the typical overlap of two different LN of a single sensitized mouse), demonstrating free and complete exchange of T_{CM} between the circulatory systems of the two mice. Prior to parabiosis, there are no shared clones in skin (lower left); only three clones are evident after parabiosis (lower right), suggesting little if any recirculation of TRM (n=3 pairs of mice). **d**, Number of shared T cell clones per 400ng tissue DNA in the LN and skin, before and after parabiosis, in three independent pairs. Experiments performed twice, representative data shown. The very small rise in the number of common sequences in skin after parabiosis may represent recirculation of a subset of skin T_{RM} ; alternatively, they could be T_{EFF} or T_{RM} generated during the common (parabiotic) life of the two animals, which would be expected to seed in the skin of both animals. n=3 pairs of mice. Values are given as mean \pm SD. **e**, Number of shared T cell clones per 400ng tissue DNA in inguinal LN of parabiotic pairs (mice H1 and H7, mice H3 and H9, mice H5 and H11). **f**, Dot plot of V β CDR3 sequences found in

the DNFB exposed skin (ear, y axis) and non-exposed skin (tail, right axis) of a DNFB sensitized mouse. In green, sequences found only in the ear; in red, sequences only found in the tail. In blue, common sequences, including a TCR defined by the CDR3 peptide CASSDRGGYNSLYF, which is highly expanded in the skin after DNFB immunization (n=3 pairs of mice). **g**, CASSDRGGYNSLYF sequence counts in tissues of both a sensitized mouse and its naïve parabiont. After parabiosis, the OT-1 clone is found at high frequency solely in the LN of both naïve and sensitized parabionts, identifying it as a T_{CM}, while its presence in the skin of only the sensitized parabiont identifies it as a T_{RM}. (n=3 pairs of mice).

Supplementary Figure 6. TCR sequence overlap in lymph nodes and skin at different ages (naïve and antigen experienced).

Experiments performed twice, representative data shown. **a**, Left panel:

Quantification of the T cell overlap (% unique T cell clone) in the cervical vs. inguinal LN in individual naïve mice (6 week old) and DNFB-sensitized mice (4 weeks post DNFB, 10 week old). Right panel: T cell overlap in the left vs. right ear in the same mice. Left y-axis, proportion of unique T cell clones observed in both samples. Right panel y-axis, proportion of total T cells observed in both samples accounting for the frequency of each unique clonotype. Naïve and sensitized mice have the same overlap in the number of unique CDR3 sequences/T cells between lymph nodes, roughly 1%. Sensitized mice have slightly more overlap between the two lymph nodes when weighted by total TCR abundance (5% vs. 7%; p = 0.031). Right panel, TCR overlap at the level of unique sequences is much higher in ears than in LN sample, and higher in sensitized than naïve mice (5% vs. 11%; p = 0.04). Sensitized mice also have substantially more overlap between the two ears when weighting by TCR abundance (20% vs. 55%; p = 0.0025) (n=3 mice for each group). **b**, Tracking of expanded ear-resident T cell clones in other tissues, naïve vs. DNFB-sensitized mice. The number of T cell clones expanded (≥ 5 T cells in 400ng of total genomic DNA) in both the left and right ears of naïve and DNFB-sensitized mice – thresholds that correspond to the selection criteria used to define such expanded clones in Figure 1. We also calculated

the mean clonal size (in T cells per 400ng gDNA) of expanded clones, and the proportion of such clones also present in tail, and in cervical and inguinal LN. In contrast to the low overlap observed among T cells between different tissues in general (1% of unique T cells, as shown above), T cell clones which are selected based on high frequency in two skin samples are likely to be found recurrently throughout the animal, and are much more abundant after sensitization than before (n=3 mice for each group). **c**, Distribution of T cell clonal abundances in 400ng of genomic DNA is shown for naïve and DNFB-sensitized mice, for skin samples (average of left ear, right ear and tail skin samples). **d**, Distribution of T cell clonal abundances in 400ng of genomic DNA is shown for naïve and DNFB-sensitized mice, for LN samples (average of cervical and inguinal LN samples). n=3 mice in each group. **e**, Distribution of T cell clonal abundances in 400ng of genomic DNA is shown for DNFB-sensitized mice, for LN samples (average of cervical and inguinal LN samples), considering only T cell clones observed at high abundance (≥ 5 cells) in at least two skin samples (with an average of 8 T cell clones matching these criteria per mouse, matching the 24 clones reported in panel b). DNFB sensitization leads to a large increase in the number of highly-expanded T cell clones detected in skin samples, and a smaller increase in the number of expanded T cell clones observed in LN samples. T cell clones at high abundance in two skin samples are much more likely to be present and highly abundant in LN samples. n=3 mice in each group. All values are given as mean \pm SD.

Supplementary Figure 7. The rapid memory response to DNFB is independent of T_{CM} migration, while the slow memory response is T_{CM} migration dependent. **a**, Sensitization and treatment scheme for each of the panels below. Experiments performed 2-3 times, representative data shown. **b**, Ratio of the peripheral blood CD3 counts in FTY-720 vs untreated mice, showing the kinetics of the lymphoid sequestration induced by FTY-720. By the 3rd day of treatment, blood levels of CD3 cells in FTY-720 treated mice were negligible, this persisted through the next four days of treatment, and began to

increase only upon cessation of treatment (n= 3 mice per group). **c**, FACS analysis of the effect of FTY-720 on CD4 and CD8 in the blood at day 3 after injection (n=6). **d**, Experimental scheme in 4a/II. Left ear swelling after challenge with DNFB mediated by adoptively transferred T_{CM} cells is blocked by pre-treatment with FTY-720, showing a dependence on migration from the lymph nodes (n= 6 mice per group). **e**, Right ear swelling after challenge with DNFB mediated by adoptively transferred T_{CM} cells is similarly blocked by the drug FTY-720 (n=6 mice per group). **f**, Experimental scheme in 4a/III. Left ear swelling after challenge with DNFB is not blocked by FTY-720, as it does not require T_{CM} migration (n=6 mice per group). **g**, Left ear thickness at indicated time points during sensitization and challenge with DNFB, in FTY-720 and vehicle treated mice, as show in (f) (n=6 mice per group). **h**, Experimental scheme 4a/IV. Left and right ear swelling after challenge with DNFB are not affected by FTY-720 (n=5 mice per group). **i**, The time to maximal left and right ear swelling after challenge with DNFB is not affected by FTY-720 (n=5 mice per group). **j**, Experimental scheme 4a/V. Mice sensitized only once but not boosted respond slowly to a late DNFB challenge, suggesting the absence of significant T_{RM} skin seeding, and a typical T_{CM} response (n=6 mice per group). **k**, Time to maximal ear swelling after DNFB challenge is prolonged in mice sensitized but not boosted (n=6 mice per group). **l**, Experimental scheme 4a/VI. Ear swelling after challenge with DNFB in mice sensitized but not boosted is FTY-720 sensitive, a finding compatible with a role for T_{CM} (n=6 mice per group). **m**, Maximal ear swelling after late challenge with DNFB in mice sensitized but not boosted is FTY-720 sensitive (n=6 mice per group). **n**, Experimental scheme 4a/VII. Kinetic of ear swelling after late DNFB challenge is affected by exposure to FTY-720 during sensitization, suggesting that T cell colonization of the skin during sensitization is essential to the rapid memory response (n=3 mice per group). **o**, Time to maximal ear swelling after DNFB challenge is prolonged in mice exposed to FTY-720 during sensitization (n=3 mice per group). All values are given as mean ± SD.

Supplementary Figure 8. T cell response kinetics of T_{RM} and T_{CM} are different yet both are long lasting.

a, Sensitization, challenge and adoptive transfer scheme. Experiments were performed twice, representative data is shown. **b**, Mice exposed to low sensitizing doses of DNFB at day 1, 2 and 7 develop a rapid (24h) ear swelling when challenged with DNFB at day 31 (n=5 mice per group). **c, d**, This rapid response is also observed when the mice are challenged at day 60 (c) or day 90 (d) respectively, demonstrating that this is a bona fide memory response. (c, n=6 per group; d, n=3 per group). **e**, Mice receiving LN-derived T cells by i.v. adoptive transfer from sensitized and boosted mice (45 days previously) also develop a significant ear swelling, yet peak swelling is attained much later (5-7 days, n=3 for naïve, 6 for sens). **f**, Time to maximal swelling takes 1 day in the sensitized mice (b, c and d), but more than 5 days in mice subjected to adoptive transfer (e, n=6 mice per group). **g**, Adoptive transfer of freshly sensitized mice (D7 post sensitization) allows for a fast response, likely due to T_{EFF} still present in the draining LN. At a later stage (D45), the LN contain only T_{CM} , and their adoptive transfer leads to a slow response, as observed in parabiotic mice (Fig 4; n=6 mice per group). **h**, Time to maximal swelling of mice shown in (g). n= 6 mice per group. All values are given as mean \pm SD.

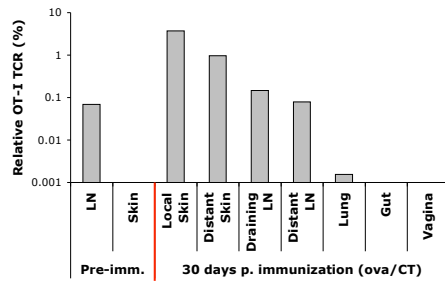
Supplementary Figure 9. Repeated antigenic skin exposure increases the intensity of the T_{RM}

response. **a**, Sensitization and challenge scheme. Experiments performed 2-3 times, representative data shown. **b**, Ear thickness after late challenge with DNFB on the left and right ear, in mice sensitized and boosted on the left ear, is highest at the skin site previously exposed to the sensitizer (left ear), although both are equally fast (n=5 mice). **c**, Ear thickness during sensitization (on the left ear), boost (on the left ear) and challenges at day 30 (on both ears), 60 (both ears) and 90 (both ears) shows progressive increase of the response intensity and kinetics matching the number of exposure, until the maximal response is obtained (n=3 mice). **d**, Ear thickness measures at precise time points before sensitization,

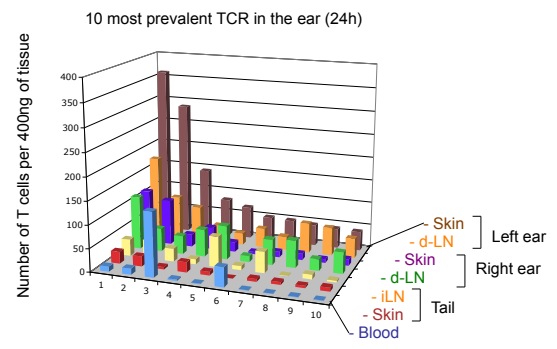
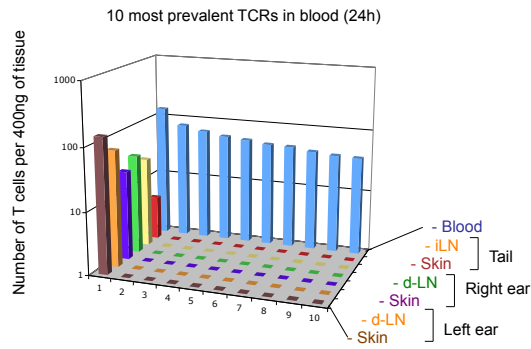
during sensitization and after each boost, as described in c. (n=3 mice). All values are given as mean \pm SD.

Supplementary Figure 10. TCR clone profiling during DPCP mediated contact dermatitis. **a**, skin samples from two different subjects share absolutely no CDR3 sequences (left panel). Within the same patient, the middle panel shows placebo treated skin (horizontal axis, red dots), day 3 post DPCP skin (vertical axis, green dots), and shared clones (blue dots). The right panel shows similar data, with placebo treated skin again on the horizontal axis (red), 4 month post DPCP skin on the vertical axis (green), and shared clones (blue). As this technique will yield false negatives but not false positives, the true number of shared TCR sequences is likely to be higher than what is shown (n=3 subjects). **b**, Dot plots of the of TCR β CDR3 sequences shared (or not) in placebo exposed or DPCP exposed skin. Several clones are present at high levels in all samples (blue box, a-c), irrespective of challenge with DPCP (placebo skin (non exposed), challenged skin at day 3, 14 and month 4). Because they are present at the four month time point in the skin, at high abundance, these T cells are likely to be T_{RM} specific for an environmental antigen encountered before the trial (not DPCP), as such abundant T_{RM} have been described before in unperturbed normal human skin¹⁶. Several clones (green box) are undetectable in placebo skin (non exposed) or challenged skin at day 3, but present at high frequency at day 14 and month 4 post challenge. These cells likely correspond to newly activated T cells recruited to the skin in response to DPCP. (n=3). **c**, Graphic representation of unrelated TRM clones (a,b,c, blue lines) and newly recruited clones (1-4, green lines); TCR counts are shown on the y axis, log scale. Clones 1-4 at 4 months also represent new TRM. (n=3).

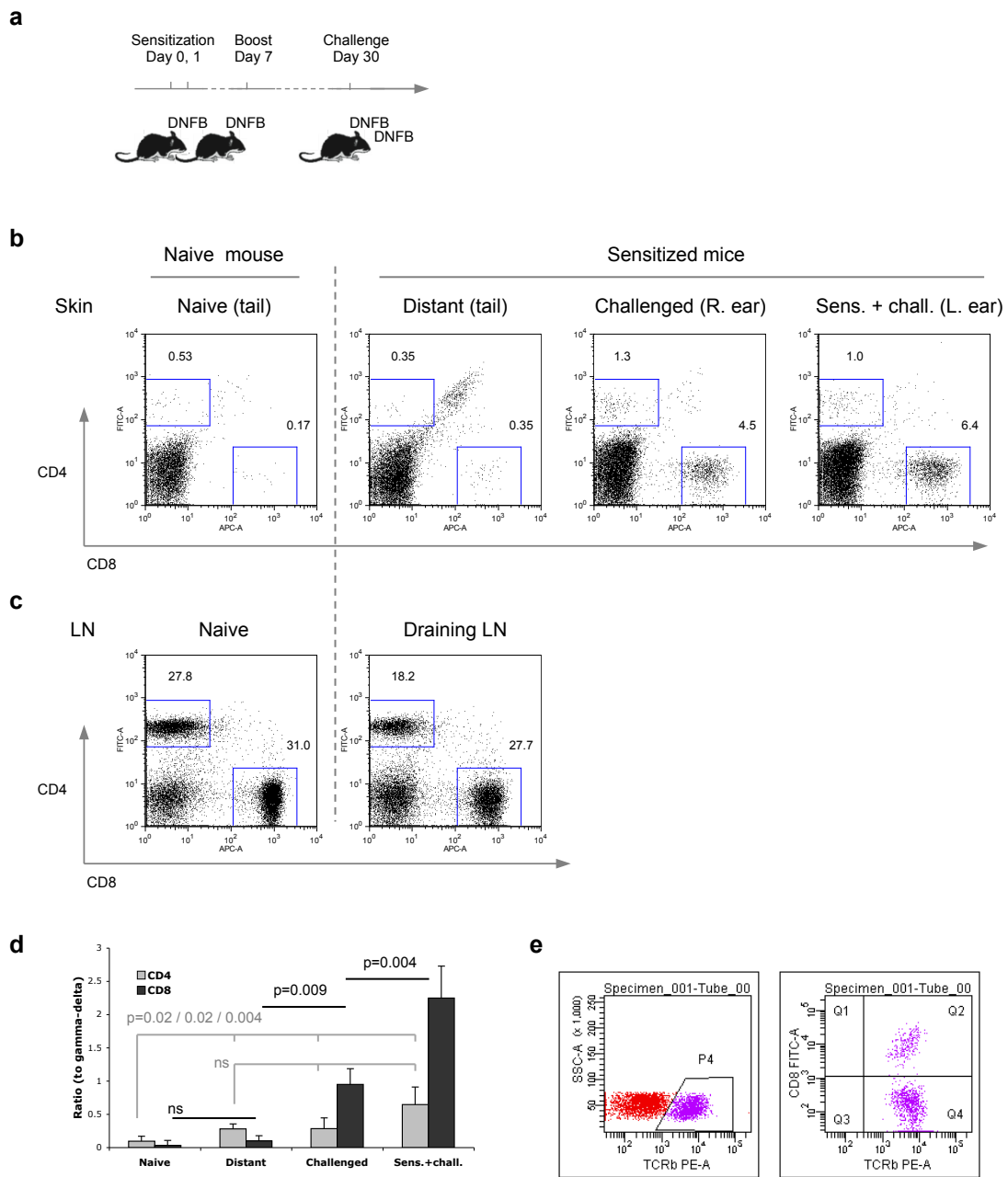
a



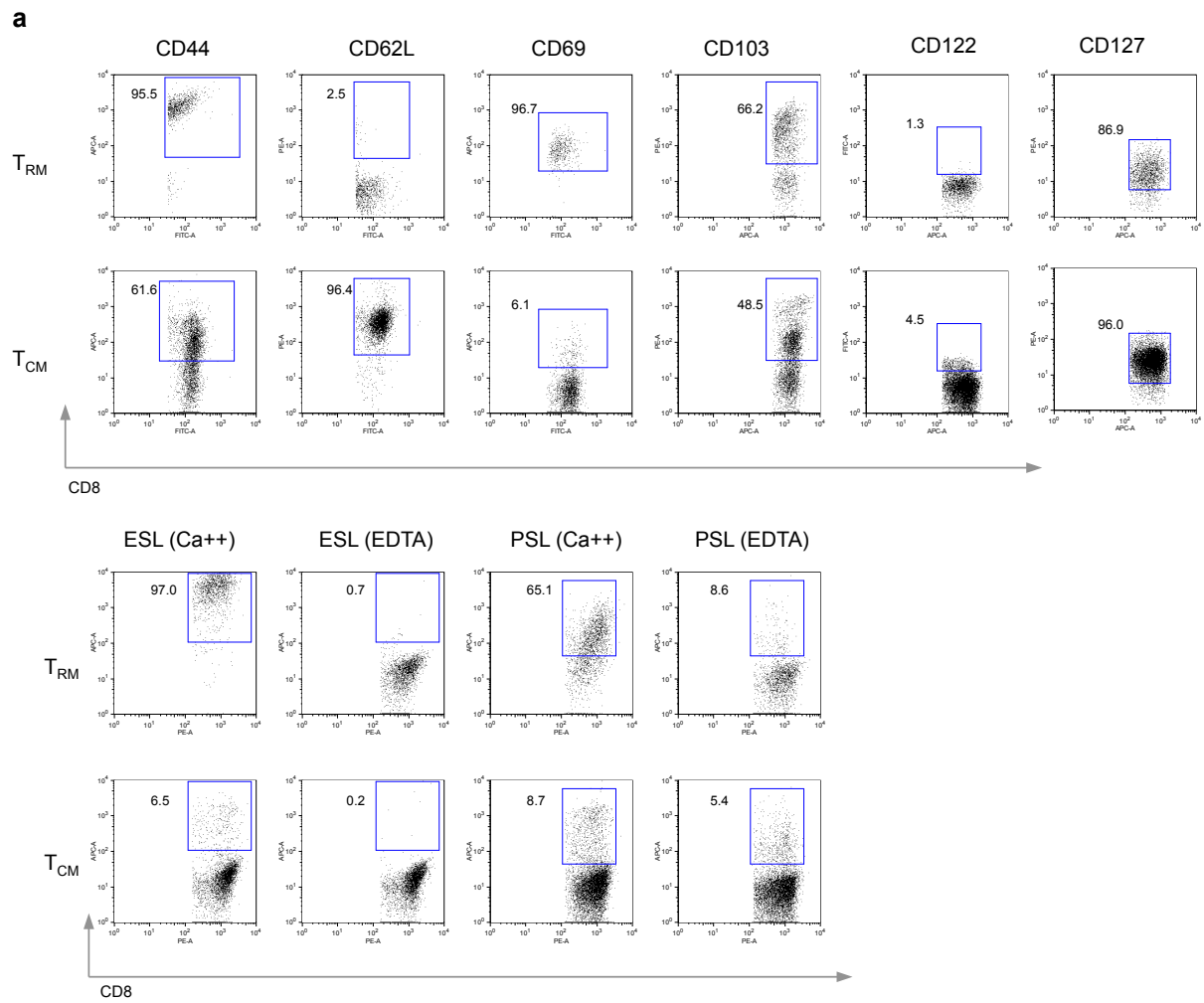
b



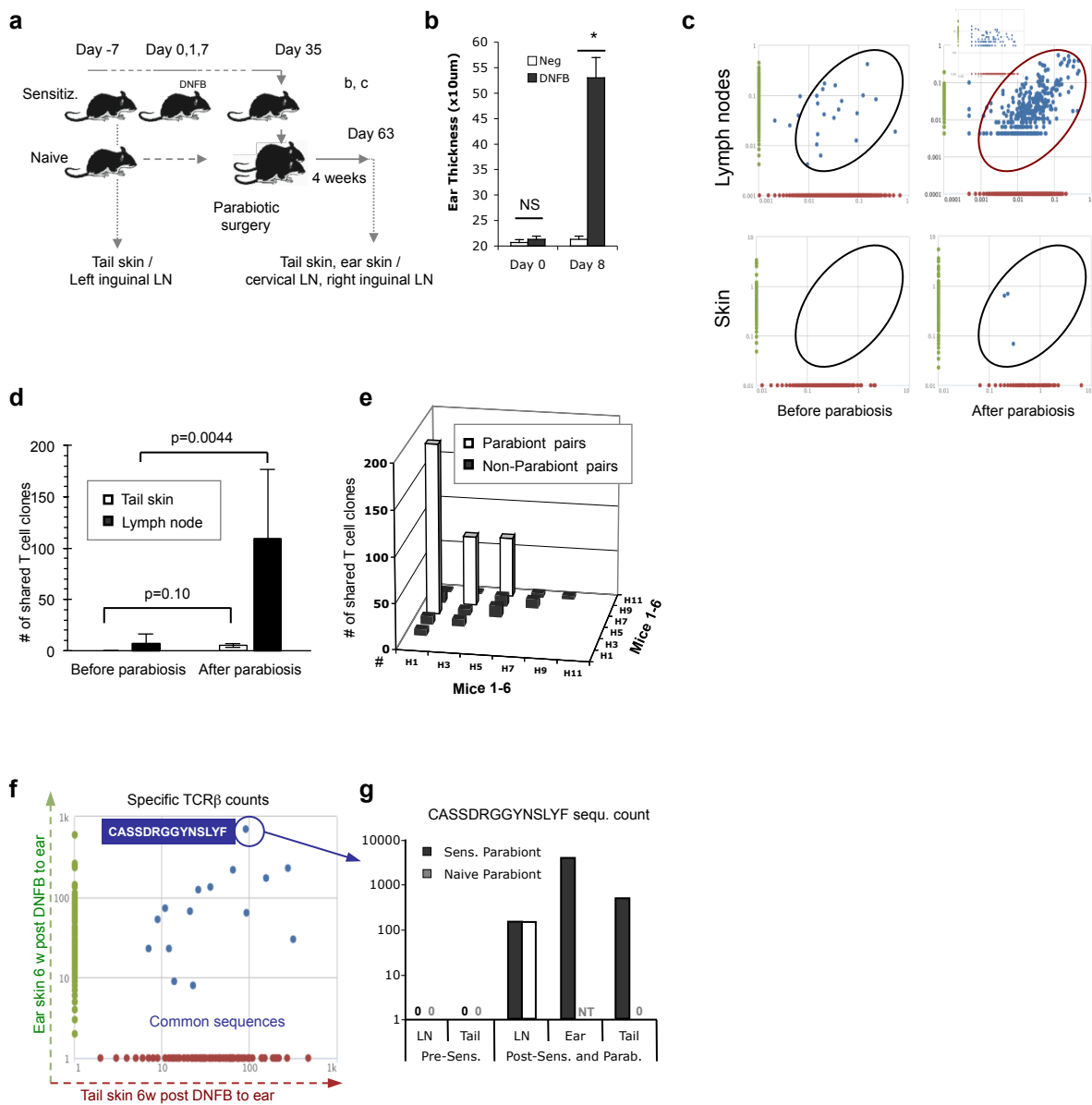
Supplementary Fig. 2. Peripheral TCR presence is not due to tissue contamination by blood T cells.



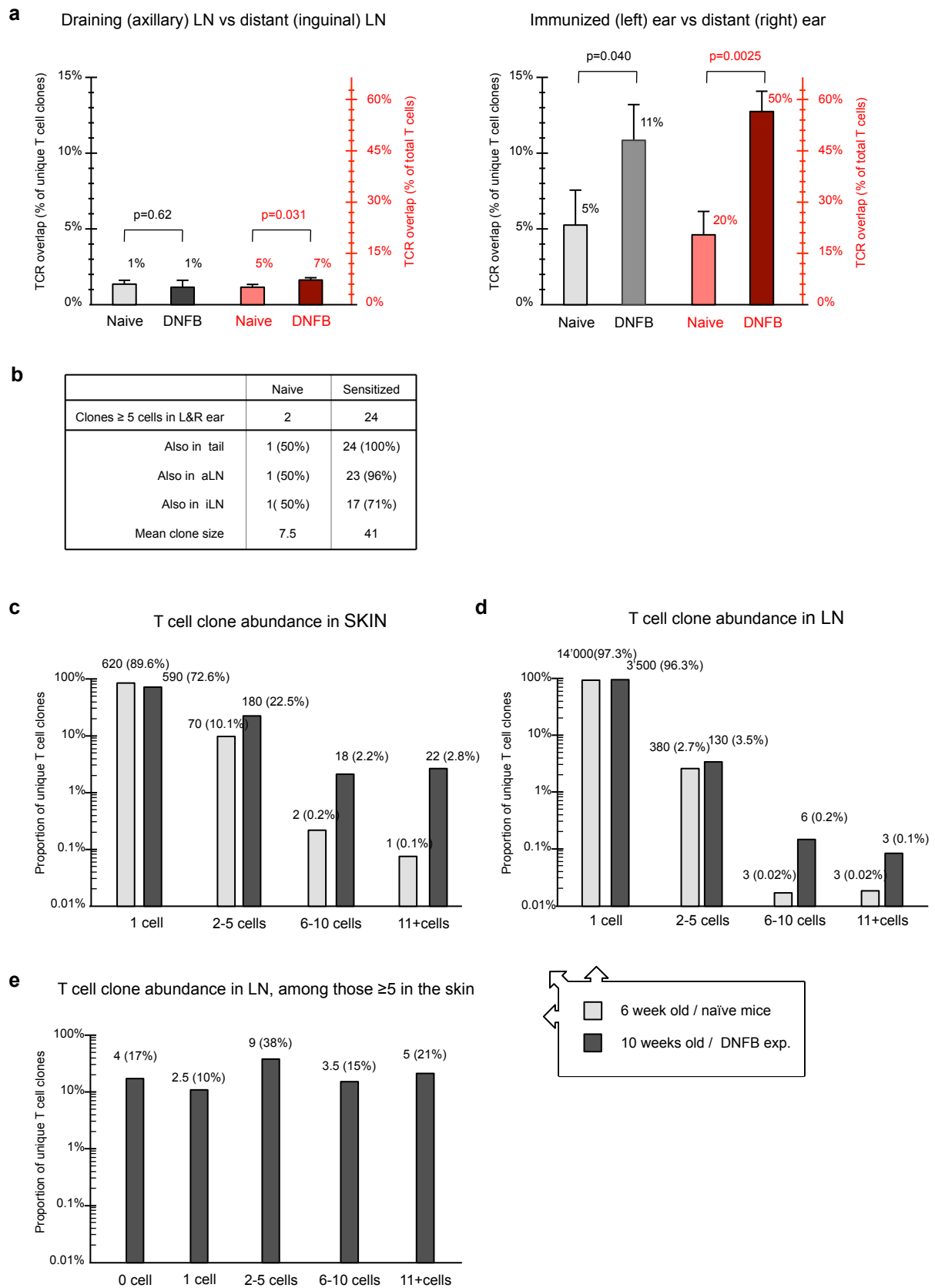
Supplementary Fig. 3. Frequency of CD4 and CD8 T cells in local and distant skin sites and LN, after multiple DNFB immunization.



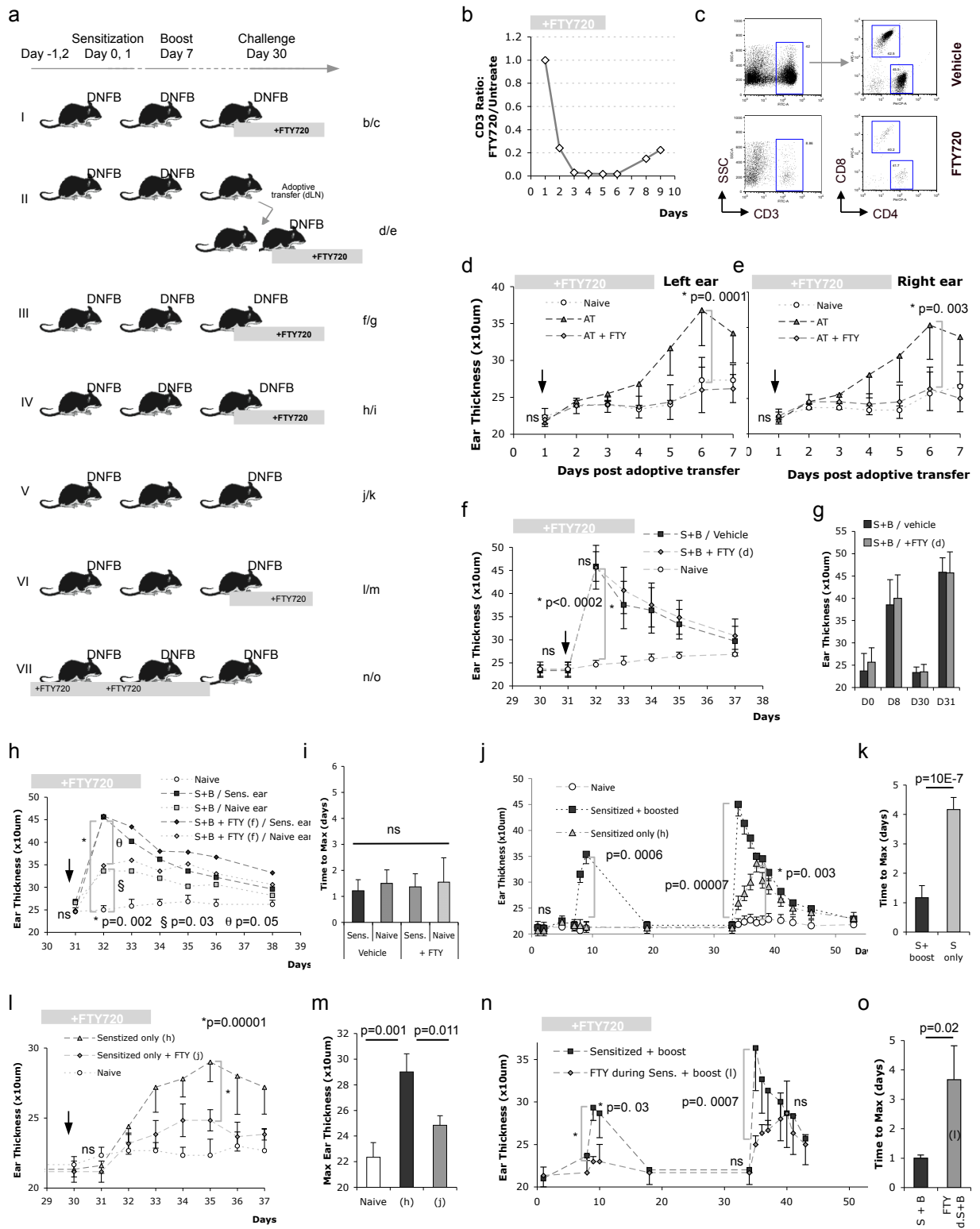
Supplementary Fig. 4. Phenotype of CD8 T cells present in LN (T_{CM}) and skin (T_{RM}) 30 days after DNFB immunization (memory phase).



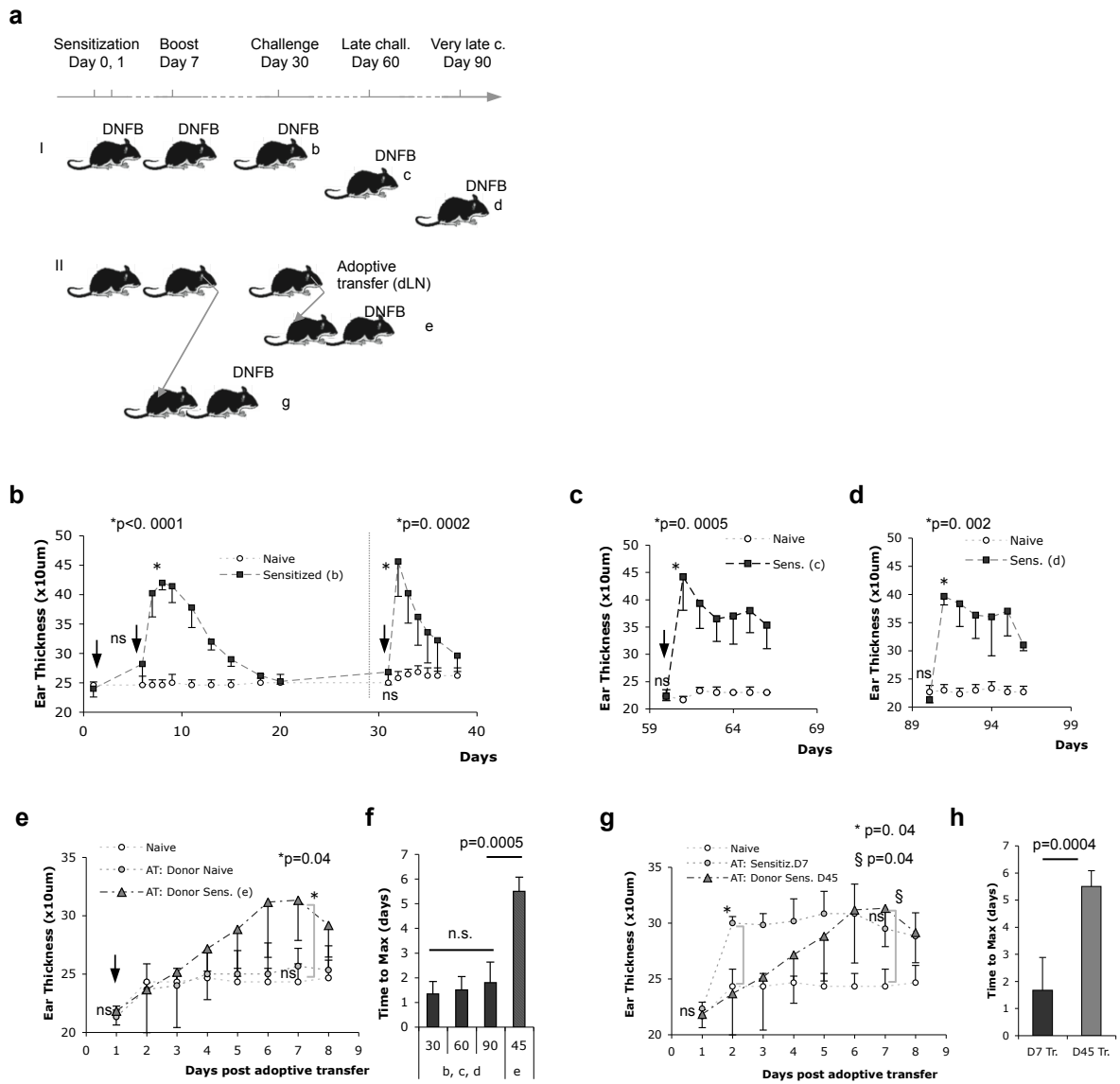
Supplementary Fig. 5. Activated naïve T cell clones give rise to both skin-resident T_{RM} and re-circulating T_{CM} .



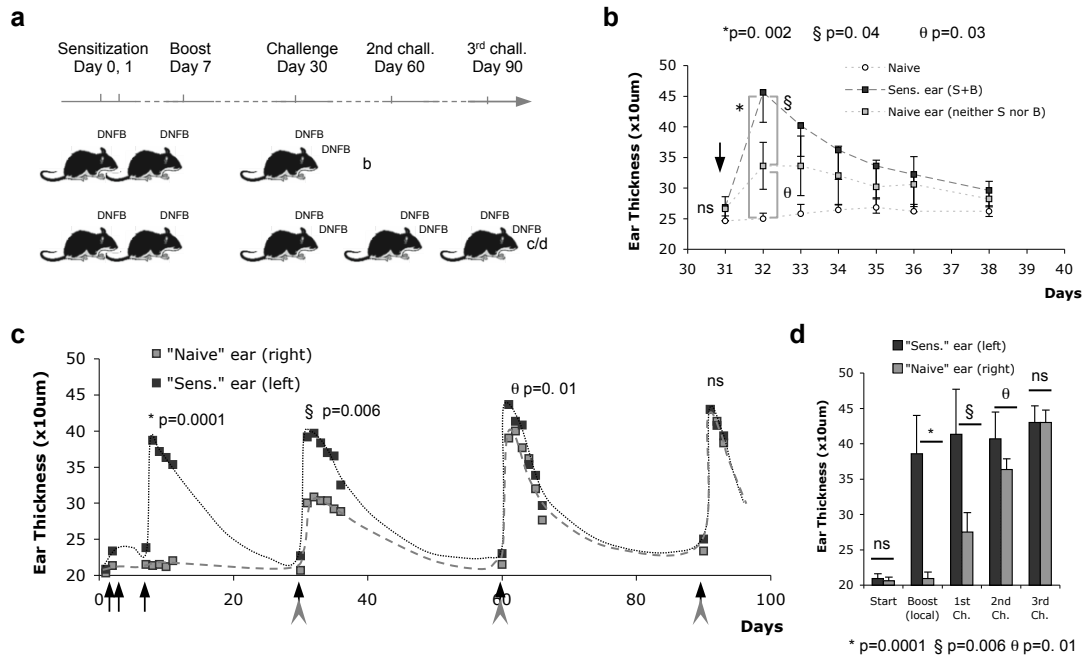
Supplementary Fig. 6. TCR sequence overlap in lymph nodes and skin at different life-stages (naïve and antigen experienced).



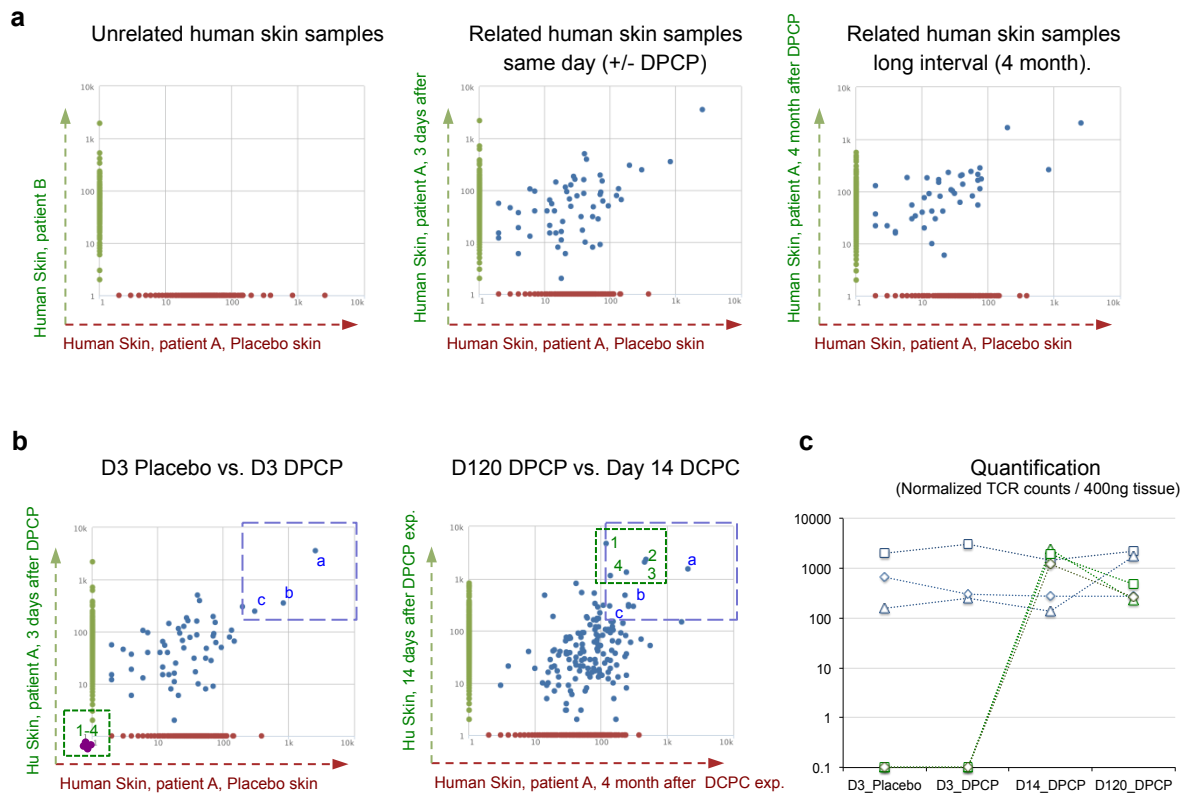
Supplementary Fig. 7. The fast memory response to DNFB is independent of T_{CM} migration, while the slow memory response is T_{CM} migration dependent.



Supplementary Fig. 8. T cell response kinetics of T_{RM} and T_{CM} are different yet both are long lasting.



Supplementary Fig. 9. Repeated antigenic skin exposure increases the intensity of the T_{RM} response.



Supplementary Fig. 10. TCR clone profiling during DPCP mediated contact dermatitis.